A Comparative Resonance Raman Analysis of Heme-Binding PAS Domains: Heme Iron Coordination Structures of the *Bj*FixL, *Ax*PDEA1, *Ec*Dos, and *Mt*Dos Proteins†

Takeshi Tomita,*,‡ Gonzalo Gonzalez,§ Alan L. Chang,§ Masao Ikeda-Saito,|| and Marie-Alda Gilles-Gonzalez*,§

Institute of Multidisciplinary Research for Advanced Materials, Tohoku University, Katahira, Aoba, Sendai 980-8577, Japan, Department of Biochemistry, Department of Plant Biology, and Plant Biotechnology Center, The Ohio State University, 1060 Carmack Road, Columbus, Ohio 43210-1002, and Department of Physiology and Biophysics, Case Western Reserve University School of Medicine, Cleveland, Ohio 44106-4970

Received October 23, 2001; Revised Manuscript Received January 31, 2002

ABSTRACT: The heme-PAS is a specialized domain with which a broad class of signal-transducing heme proteins detect physiological heme ligands. Such domains exhibit a wide range of ligand binding parameters, yet they are all expected to feature an α−β heme binding fold and a predominantly hydrophobic heme distal pocket without a distal histidine. We have compared, for the first time, the resonance Raman spectra of several heme-PASs: the heme-binding domains of *Bradyrhizobium japonicum* FixL, *Escherichia coli* Dos, *Acetobacter xylinum* PDEA1, and *Methanobacterium thermoautotrophicum* Dos. In all cases, the ν_{Fe-CO} and ν_{C-O} values of the carbonmonoxy forms were consistent with coordination of the heme iron to histidine on the proximal side and binding of the CO without electrostatic interaction with the heme distal pocket. *Ec*Dos was unusual in having predominantly hexacoordinate heme iron in the deoxy and met forms. Despite an evident lack of CO interaction with the *Ec*Dos heme pocket, relatively low Fe−O_2 (562 cm^{-1}) and N−O (1576 cm^{-1}) stretching frequencies indicated that strong polar interactions with that heme distal pocket are possible for highly bent ligands such as O_2 or NO. None of the newly studied NO adducts exhibited evidence of the Fe−His rupture and pentacoordination previously noted for *Sinorhizobium meliloti* FixL. A low Fe−His stretching frequency, formerly interpreted as a strained Fe−His bond, and the slow association of O_2 with *S. meliloti* FixL failed to correlate with the newly studied proteins having low association rate or low equilibrium association constants for binding of O_2. We conclude that although heme-PASs share some features, they represent distinct signal transduction mechanisms.

PAS[1] domains are structural modules characterizing a family of sensory proteins that occur in bacteria, archaea, and eukaryotes (*1*). A subgroup of these domains, the heme-PASs, contain heme and function as sensors of heme ligands (*2*). In every case, the coordination status of the iron atom in the heme-PAS regulates a distinct enzymatic domain in the same protein. Heme-PASs are ∼50% homologous in sequence, occupy one-third to one-fourth of the total protein sequence within which they occur, and always precede the enzymatic domain (*2*). In *Sinorhizobium meliloti* FixL, *Bradyrhizobium japonicum* FixL, and *Methanobacterium thermoautotrophicum* Dos, the heme-regulated enzymatic domain is a histidine protein kinase (*3*−*5*). In *Acetobacter xylinum* PDEA1 and *Escherichia coli* Dos, the enzymatic domain is a phosphodiesterase that linearizes a cyclic dinucleotide second messenger (*6*). On the basis of the crystal structures of the O_2-sensing domain of FixL proteins, it is clear that heme-PASs are quite unlike hemoglobins or cytochromes (*7*, *8*). A striking difference is that in heme-PASs, the heme is held between five antiparallel β-strands on the distal side and an α-helix on the proximal side. To facilitate comparison of key residues and structural features of heme-PASs, a nomenclature analogous to that of hemoglobin has been established for the amino acid residues (*7*).

The absorption spectra of heme-PASs suggest that, even when lacking an exogenous heme ligand, for example, in the met and deoxy forms, there are differences in heme iron coordination (*9*, *12*). Not surprisingly, these domains display

† This research was supported by National Science Foundation Grant MCB-9724048, U.S. Public Health Service Grants HL-64038 and GM-57272, and Grants-in-Aid (12480176 and 12147201) from the Ministry of Education, Science, Technology, Culture, and Sports, Japan.

* To whom correspondence should be addressed. T.T.: phone, +81-22-217-5117; fax, +81-22-217-5118; e-mail, tomigc@tagen.tohoku.ac.jp. M.-A.G.-G.: phone, (614) 688-3303; fax, (614) 688-3302; e-mail, gilles-gonzalez.1@osu.edu.

‡ Tohoku University.

§ The Ohio State University.

|| Case Western Reserve University School of Medicine.

[1] Abbreviations: PAS, sensory domain with an α−β fold named after the eukaryotic proteins period, arnt, and simple-minded; heme-PAS, heme-binding PAS domain; *Ax*PDEA1, *A. xylinum* phosphodiesterase A1; *Ax*PDEA1H, *A. xylinum* phosphodiesterase A1 heme-PAS; *Bj*FixL, *B. japonicum* FixL; *Bj*FixLH, *B. japonicum* FixL heme-PAS; Dos, direct oxygen sensor; *Ec*Dos, *E. coli* Dos protein; *Ec*DosH, *E. coli* Dos heme-PAS; *Mt*Dos, *M. thermoautotrophicum* Dos protein; *Mt*DosH, *M. thermoautotrophicum* Dos heme-PAS; *Rm*FixL, *S. meliloti* (formerly *Rhizobium meliloti*) FixL; *Rm*FixLH, *S. meliloti* FixL heme-PAS; *Rm*FixLT, *S. meliloti* truncated FixL containing the heme-PAS followed by a histidine protein kinase domain; Hb R, relaxed state of hemoglobin; Hb T, tense state of hemoglobin; SW Mb, sperm whale myoglobin; ν_{Fe-His}, Fe−histidine stretching mode; ν_{Fe-CO}, Fe−CO stretching mode; ν_{C-O}, C−O stretching mode; δ_{Fe-C-O}, Fe−C−O bending mode; ν_{Fe-O}, Fe−O_2 stretching mode; ν_{Fe-NO}, Fe−NO stretching mode; ν_{N-O}, N−O stretching mode; deoxy, Fe^{II} heme protein without an exogenous ligand; met, Fe^{III} heme protein without an exogenous ligand. For liganded heme proteins: carbonmonoxy, Fe^{II}-CO; oxy, $Fe^{II}O_2$; nitrosyl, $Fe^{II}NO$; imidazolemet, Fe^{III}imidazole.

10.1021/bi0158831 CCC: $22.00
Published on Web 03/21/2002

a broad range of parameters for binding of ligands such as O_2, CO, NO, CN^-, and imidazole (*2*, *6*, *9*−*12*). Nonetheless, a few generalizations can be made. First, on the basis of structural studies and mutagenesis, the site of heme coordination in heme-PASs is expected to be the conserved histidine $F_\alpha 3$ (*7*, *8*, *13*, *14*). Second, their heme-binding pockets lack the distal histidine (histidine E7 of hemoglobin) commonly found in O_2-binding heme proteins. Instead, the only residue known to stabilize a bound ligand by hydrogen bonding is the $G_\beta 2$ arginine (*15*). This residue is conserved in all the proteins discussed in this report, except *Mt*Dos. Third, in at least the FixL proteins, the heme-binding pockets impose essentially no steric hindrance to the entrance of ligands. This is most apparent from the rapid and tight binding of bulky ligands such as imidazole (*10*, *11*).

Among the heme-controlled histidine kinases, the best-studied regulatory mechanisms are the heme-PASs belonging to the FixL proteins. The FixL proteins direct the hypoxic expression of nitrogen-fixation genes in *Rhizobia* (*2*, *3*, *16*, *17*). These proteins have extremely slow O_2 association rates ($k_{on} \sim 10^{-1}$ μM^{-1} s^{-1}) (*9*). For *S. meliloti* deoxy-FixL (*Rm*FixL), the Fe−His stretching frequency is unusually low (209 cm^{-1}), even lower than that of T-state hemoglobin (*18*−*20*). The comparably low association rate constants for binding of O_2 to T-state hemoglobin have led to a notion that a low ν_{Fe-His} correlates with slow O_2 on-rates to some extent (*21*). Study of additional proteins should help to verify whether such correlations are justified for heme-PAS proteins. The recently discovered *Mt*Dos protein is an archaeal histidine kinase related to the FixL proteins. *Mt*Dos is the first heme-PAS protein from an archaeon and so far the only thermostable heme protein for which reversible O_2 binding has been examined.

The *Ax*PDEA1 and *Ec*Dos proteins are heme-controlled phosphodiesterases. *Ax*PDEA1 regulates the production of a buoyant cellulose pellicle by *A. xylinum*, an organism best known for its abundant synthesis of highly pure and microcrystalline cellulose (*22*). Association of O_2 with *Ax*PDEA1 ($k_{on} \sim 6.5$ μM^{-1} s^{-1}) is considerably faster than with FixL proteins and much more similar to the behavior of myoglobin (*2*, *6*). The *Ec*Dos protein of *E. coli* is similar in sequence to *Ax*PDEA1 (*12*). *Ec*Dos is unique among the known heme-PAS proteins in having absorption spectra that suggest hexacoordination of the heme iron in the absence of exogenous ligands (*12*). Thus, in addition to a proximal histidine expected for all heme-PASs, the *Ec*Dos heme distal pocket appears to supply a residue that functions as the sixth axial ligand of the heme iron. This residue, probably the unique methionine FG8 of *Ec*Dos, is readily displaced by O_2, CO, or NO (*12*).

Though O_2 and CO binding characteristics have been reported for all but the *Mt*Dos protein, structural data are available for only the heme-PAS from the histidine kinases *Bj*FixL and *Rm*FixL. For *Bj*FixLH, crystal structures are available for the oxy, met, cyanomet, and imidazolemet forms, but vibrational spectroscopic data have not yet been reported for any form (*7*, *15*). For *Rm*FixLH, crystal structures are limited to the unliganded forms (deoxy and met), but resonance Raman data are available for unliganded as well as liganded forms (*8*, *23*−*27*). Resonance Raman spectroscopy is an excellent method for elucidating details of the heme structure. It is now well established that some porphyrin skeletal vibrations are representative of the coordination and spin state of the heme. Raman bands of ligands coordinated to the heme iron are also detectable when the excitation wavelength is appropriately chosen (*28*). On the basis of many studies of heme proteins and model compounds, the electronic state of heme iron can be analyzed clearly. More importantly, we can examine interactions of the bound ligand (CO, NO, O_2, and so on) with amino acids around heme, based on the Raman band positions for the found ligand bound. This information is very important for understanding what occurs in a sensory heme-binding domain when the ligand triggers an on or off switch. In other words, resonance Raman data can provide basic knowledge of the mechanism for O_2 recognition and for communication of O_2 binding. Here we examine the resonance Raman spectra of the deoxy, met, oxy, nitrosyl, and carbonmonoxy forms of four different heme-PASs, two of which are derived from kinases and two from phosphodiesterases. This work establishes the features that are characteristic of this novel type of heme-binding pocket and the ones that are specific to a given protein.

EXPERIMENTAL PROCEDURES

Gene Expression and Protein Purification. Overproduction and purification of PAS-domain proteins have previously been reported (*6*, *9*, *12*). Briefly, the heme-binding domains were overproduced in *E. coli* from gene segments encoding the corresponding PAS domains. Expression of the plasmid-borne genes from a *tac* promoter was induced by adding isopropyl β-D-glucopyranoside (500 μM) to exponentially growing TG1 cells. After induction for 4−5 h at 37 °C, the cells were cooled to 4 °C and harvested. The cell pellets were stored at −70 °C until the protein purifications were carried out. All subsequent protein manipulations were carried out at 0−4 °C. A "standard buffer" containing 50 mM Tris-HCl (pH 8.0), 50 mM NaCl, and 5% glycerol was augmented as indicated below. All column matrices were from Pharmacia. Cleared lysates were obtained by centrifuging cells ruptured by sonication for 3 min. Proteins were purified from those cleared lysates by ammonium sulfate precipitation (1.6 and 2.4 M ammonium sulfate) followed by desalting (Sephadex G25), ion-exchange fractionation (DEAE-Sephacel, 50 to 150 mM NaCl gradient), and gel filtration (Superdex 75). Following purification, the proteins were stored at −70 °C in the standard buffer. Protein purity was verified from the 250−700 nm absorption (UV/Soret absorbance ratio) of the met forms and Coomassie brilliant blue staining of the purified proteins after their electrophoresis on SDS−polyacrylamide gels (15% acrylamide gels, Laemmli system).

Resonance Raman Measurements. Raman spectra were obtained with the 413.1 nm line of a krypton ion laser (Spectra Physics) or the 441.6 nm line of a He−Cd laser (Kinmon Electronics). Raman spectra were detected by a CCD camera attached to a single polychromator (Ritsu Oyokogaku, DG-1000). The sample concentration was 50 μM in 50 mM potassium phosphate (pH 7.0). The sample temperature was 20 °C. Unless otherwise stated, for all measurements, the laser power was 2 mW and the accumulation time was 5 min. The sample solution (0.1 mL) was placed in an airtight spinning cell with a rubber septum, and the headspace was substituted by nitrogen with repetitions

Table 1: Heme Iron Coordination in the Heme-PAS without an Exogenous Ligand and Raman Frequencies of Porphyrin Skeletal Modes for Heme-PASs

protein	coordination[a]	ν_4 (cm^{-1})	ν_3 (cm^{-1})	ν_2 (cm^{-1})	ν_{10} (cm^{-1})
oxidized (met, Fe^{III})					
*Bj*FixLH	5-c HS	1370	1493	1562	1628
*Ax*PDEA1H	6-c LS/5-c HS[b]	1372	**1503**/1493	1577	1640/1628
*Ec*DosH	6-c LS	1370	1505	1576	1639
*Mt*DosH	5-c HS/6-c LS[c]	1372	**1495**/1505	1568	1630/1640
reduced (deoxy, Fe^{II})					
*Bj*FixLH	5-c HS	1353	1469	1555	1602
*Ax*PDEA1H	5-c HS	1354	1469	1557	1607
*Ec*DosH	6-c LS	1361	1493	1580	1625
*Mt*DosH	5-c HS	1354	1469	1561	1606

[a] Heme iron coordination: 5-c, pentacoordinate; 6-c, hexacoordinate; HS, high-spin; LS, low-spin. [b] For met-AxPDEA1H, 6-c LS is dominant. [c] For met-MtDosH, 5-c HS is dominant.

of degassing and filling with pure nitrogen gas. The samples were reduced with sodium dithionite. The CO- and NO-bound forms were prepared by introducing the respective gases into the headspace of the cell. The O_2-bound forms were prepared by addition of a dithiothreitol solution (final concentration of 10 mM) and then flushing the sample cell with pure O_2. Raman spectra were calibrated with indene and CCl_4, and the spectral accuracy is within ± 1 cm^{-1}.

Rate Constants for Imidazole Association. The rates of binding of imidazole were measured with an Applied Photophysics (Leatherhead, U.K.) SX17MV reaction analyzer with a dead time of 2 ms. All reactions had 2−8 μM heme-PAS in 100 mM Tris-HCl (pH 8.0) at 25 °C. Imidazole concentrations ranged from 0.025 to 5.0 mM in 100 mM Tris-HCl (pH 8.0). The apparent rate constants (k_{obs}) were obtained by following the absorption versus time at 418 nm, i.e., the wavelength of maximum difference between the liganded and unliganded met species. Association rate constants (k_{on}) were obtained from the linear region of the plot of k_{obs} versus ligand concentration. For every ligand concentration, a minimum of three k_{obs} were averaged, each of which fits a single exponential. Each k_{on} was calculated from the slope of k_{obs} versus concentration, for five ligand concentrations spanning a wide range. All r^2 values for these lines were >0.99.

RESULTS AND DISCUSSION

Spin and Coordination of the Heme Iron in Deoxy and Met Forms of the Proteins. In Soret-excited resonance Raman spectra, the readily observable Raman bands ν_4, ν_3, and ν_{10} in the 1300−1750 cm^{-1} region are highly sensitive to the coordination structure and spin state of heme iron. The resonance Raman spectra in this region for the deoxy forms (Fe^{II}) of the heme-PAS proteins and their respective met forms (Fe^{III}) are shown in Figure 1A and summarized in Table 1. The deoxy forms of the *Bj*FixLH (a), *Ax*PDEA1H (b), and *Mt*DosH (d) proteins had pentacoordinate high-spin ferrous heme iron, as indicated by the occurrence of ν_4, ν_3, and ν_{10} in the range of 1353−1354, 1469, and 1602−1607 cm^{-1}, respectively. These results are similar to the previously measured resonance Raman spectra of *Rm*FixLH and consistent with the crystal structure of this heme-PAS (*18*, *24*). In contrast, the deoxy-*Ec*DosH (c) ν_4, ν_3, and ν_{10} values of 1361, 1493, and 1625 cm^{-1}, respectively, indicated a hexacoordinate low-spin heme iron. Among the met forms of the heme-PASs, *Bj*FixLH (e) was the only one with

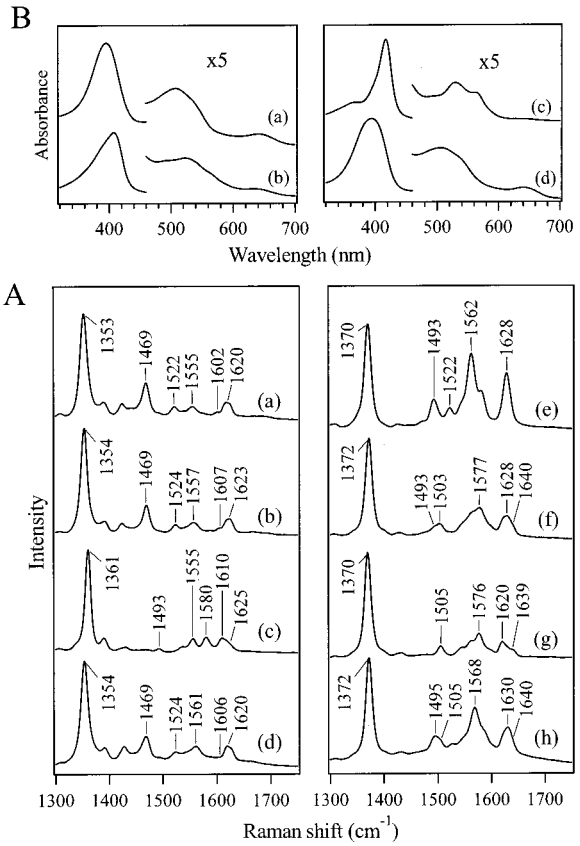

FIGURE 1: Heme iron coordination in heme-PAS proteins. (A) The left panel shows the resonance Raman spectra for the reduced (deoxy, Fe^{II}) forms of *Bj*FixLH (a), *Ax*PDEA1H (b), *Ec*DosH (c), and *Mt*DosH (d); the right panel shows spectra of the oxidized (met, Fe^{III}) forms of *Bj*FixLH (e), *Ax*PDEA1H (f), *Ec*DosH (g), and *Mt*DosH (h). Panel B shows the absorption spectra of the oxidized forms of *Bj*FixLH (a), *Ax*PDEA1H (b), *Ec*DosH (c), and *Mt*DosH (d).

exclusively pentacoordinate ferric heme iron. This heme iron coordination agrees with the crystal structures of *Bj*FixLH and *Rm*FixLH and with the resonance Raman data reported for *Rm*FixLH (*7*, *8*, *24*). In contrast, predominantly hexacoordinate heme iron was indicated for met-*Ec*DosH (g) and a mixture of hexa- and pentacoordinate heme iron for met-*Ax*PDEA1H (f) and met-*Mt*DosH (h). Since the ν_3 bands at 1493 and 1503−1505 cm^{-1} are characteristic of pentacoordinate high-spin heme iron and hexacoordinate low-spin heme iron, respectively, the dominant species in met-*Ax*PDEA1H is hexacoordinate low-spin heme and in met-

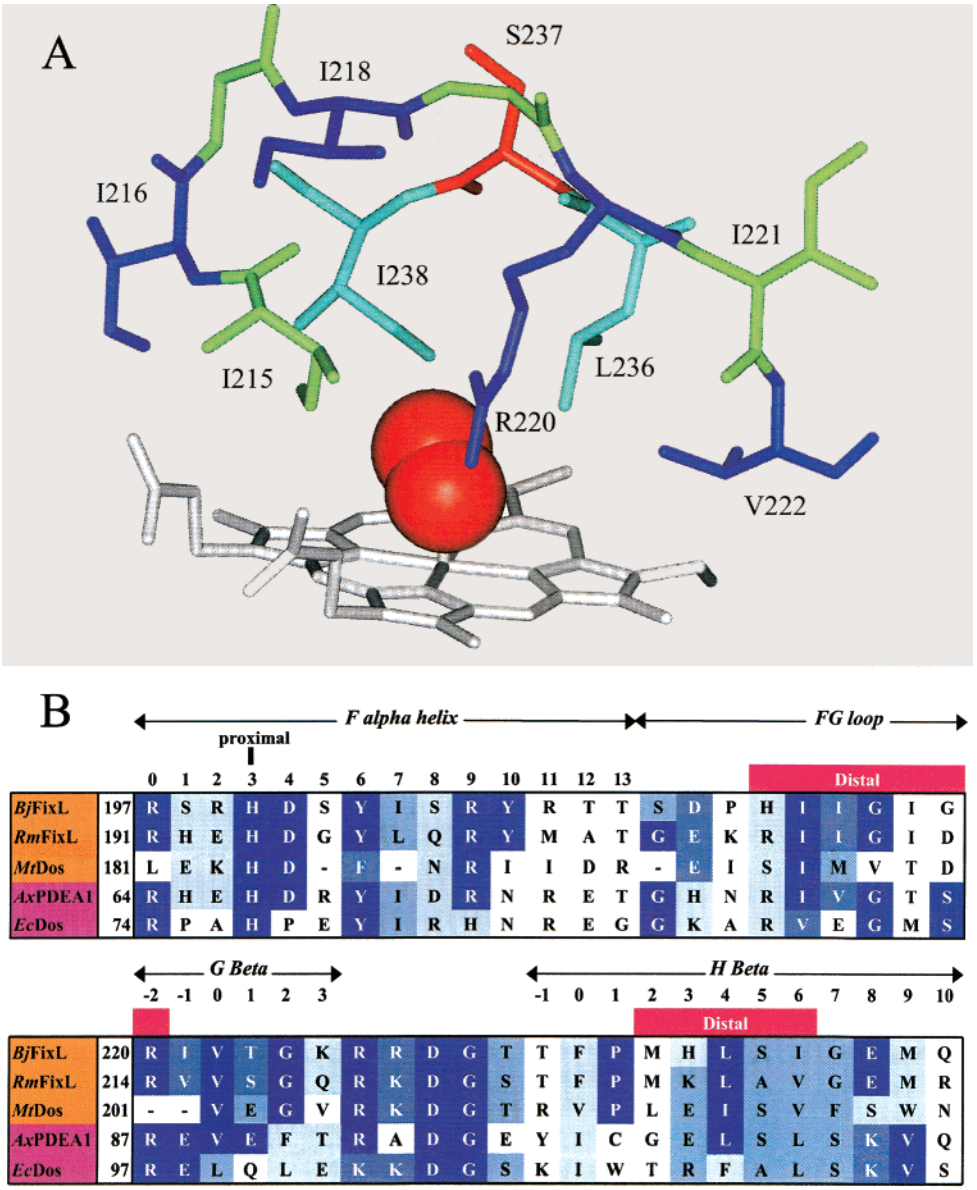

FIGURE 2: Heme pocket regions of heme-PAS proteins. Panel A shows the structure of the heme distal pocket in oxy-*Bj*FixLH, illustrating the stabilization of bound O_2 by the G_β-2 arginine (Arg220) (*15*). Panel B shows a secondary structure alignment for the entire heme pocket regions of *Bj*FixL, *Rm*FixL, *Mt*Dos, *Ax*PDEA1, and *Ec*Dos. In *Ec*Dos, a phenylalanine at position $H_\beta 4$ (Leu236 in *Bj*FixL) may stabilize the bound O_2, and a methionine at position FG8 (Ile218 in *Bj*FixL) coordinates to the heme iron on the distal side.

*Mt*DosH is pentacoordinate high-spin heme. The optical absorption spectra are consistent with the conclusions drawn from resonance Raman spectroscopy (Figure 1B) (*6*, *9*, *12*). For example, the absorption spectrum of met-*Ec*DosH (Figure 1B, c) featured α and *β* bands in the 500−600 nm region that are characteristic of low-spin ferric heme and a sharp Soret band at ∼418 nm. The spectrum of met-*Ax*PDEA1H (Figure 1B, b) had a Soret peak at 408 nm (97 mM^{-1}), being characteristic of the presence of the sixth ligand, but a broad absorption band around 390 nm indicates that there is a substantial amount of pentacoordinate high-spin heme iron. The absorption spectrum of met-*Mt*DosH (Figure 1B, d), on the other hand, featured a quite symmetric band at 394 nm (117 mM^{-1}) and was very similar to that of *Bj*FixLH (Figure 1B, a). Hence, only small fraction of the *Mt*DosH heme iron is hexacoordinate, although this was sensitively detected by resonance Raman spectroscopy.

In all cases, the resonance Raman spectra were consistent with the fifth axial ligand of the heme iron being a neutral imidazole side chain (see the discussions of the iron−histidine stretch and CO binding below). The histidine of coordination is expected to be the highly conserved histidine $F_\alpha 7$, demonstrated to be the site of the heme iron attachment in two different FixL proteins (His200 in *B. japonicum* FixL and His194 in *S. meliloti* FixL) (*7*, *8*). With regard to the sixth axial ligand, structural modeling based on FixL suggests that the only residues of the heme distal pocket that could potentially coordinate to the heme iron are the $G_\beta 1$ arginine and an FG-loop methionine (Figure 2). The $G_\beta 1$ arginine occurs in all the heme-PASs in this study except *Mt*DosH. There is not yet any model of coordination of a guanido group to heme iron for spectroscopic comparisons. The distal methionine occurs in *Ec*DosH and *Mt*DosH at positions FG8 and FG6, respectively. For met-*Ec*DosH, ligation of the heme

iron to the methionine sulfur is supported by magnetic circular dichroism and mutagenesis data (unpublished results of M. Cheesman, N. Watmough, G. Gonzalez, and M.-A. Gilles-Gonzalez). For met-*Ax*PDEA1H and met-*Mt*DosH, the sixth axial ligand is not yet known.

The porphyrin ring in isolated heme is essentially flat; however, insertion into the protein causes significant out-of-plane distortions in the porphyrin that are believed to modulate properties such as redox potential and ligand affinity. These out-of-plane distortions vary widely with the type of heme protein and the coordination of the heme. In *Bj*FixL, the out-of-plane distortion known as "ruffling" or b1u is reduced by 0.4 Å upon changing from pentacoordinate high-spin to hexacoordinate low-spin heme. This change in heme shape, which has been somewhat imprecisely termed "flattening", has been proposed as the basis of heme-mediated ligand sensing in *Bj*FixL (*4*, *7*). In the case of *Ec*Dos, protein conformational change (in the form of displacement of the distal residue) is intrinsically necessary for ligand binding, and there is no need to seek an indirect, porphyrin-driven mechanism for altering protein conformation (*12*). It has been argued that since *Ec*Dos is hexacoordinate even before it binds O_2, the mechanism proposed for FixL cannot contribute to ligand-driven conformational changes in *Ec*Dos. However, it is possible that significant changes in porphyrin shape could be driven by the replacement of the sixth ligand of *Ec*Dos, without requiring a change in coordination number. Determination of the three-dimensional structures for active and inactive forms of *Ec*Dos and other heme-PASs will help to clarify their ligand-induced protein conformational changes.

The Iron−Histidine Stretch. Excitation at 441.6 nm is often exploited to reveal the Fe−His stretching frequency (ν_{Fe-His}) of pentacoordinate ferrous heme. For O_2-binding heme proteins, the ν_{Fe-His} values typically range from 200 to 220 cm^{-1}. A low ν_{Fe-His} is thought to have some correlation with diminished affinity for O_2 (*21*). Thus, the relatively low Fe−His frequency of deoxy-*Rm*FixLH (209 cm^{-1}) could be proposed to account for its low association rate and equilibrium association constants for binding O_2 (*18*, *21*). Our comparative study of heme-PAS proteins finds no correlation between their ν_{Fe-His} and O_2 binding parameters and no support for the premise that a low ν_{Fe-His} is a general feature of O_2 sensing (Figure 3 and Table 2). For example, deoxy-*Ax*PDEA1 (b) had relatively rapid O_2 association and high O_2 affinity, although its ν_{Fe-His} (212 cm^{-1}) was as low as that of *Rm*FixLH (*6*). Deoxy-*Bj*FixLH (a) had association rate and equilibrium association constants for O_2 binding that were even lower than those of *Rm*FixLH, despite having a ν_{Fe-His} (217 cm^{-1}) typical of myoglobins (*9*). Deoxy-*Mt*DosH (d) also has the same ν_{Fe-His} (218 cm^{-1}). As expected from the hexacoordinate heme iron structure of deoxy-*Ec*DosH (c), a ν_{Fe-His} stretching mode was absent from the resonance Raman spectrum.

Binding of CO. Because of the sensitivity of the Fe−CO and the C−O stretching frequencies to the heme environment, the CO adducts of heme proteins provide a valuable probe of the heme pocket. The low- and high-frequency region resonance Raman spectra for the CO complexes of *Bj*FixLH (a), *Ax*PDEA1H (b), *Ec*DosH (c), and *Mt*DosH (d) are shown in Figure 4A and summarized in Table 3. There is a well-established inverse correlation between ν_{C-O} and

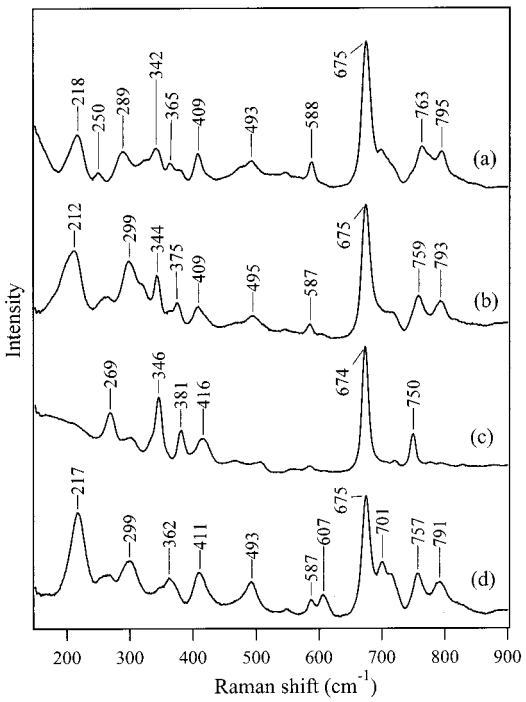

FIGURE 3: Iron−histidine stretch of heme-PAS proteins. Resonance Raman spectra are shown in the 200−900 cm^{-1} region for the deoxy forms of *Bj*FixLH (a), *Ax*PDEA1H (b), *Ec*DosH (c), and *Mt*DosH (d). The resonance Raman excitation was at 441.6 nm.

Table 2: Fe−His Stretching Frequencies and Parameters for O_2 and Imidazole Binding to the Heme-PAS

protein	ν_{Fe-His} (cm^{-1})	$K_d(O_2)$[a] (μM)	$k_{on}(O_2)$ (μM^{-1} s^{-1})	$k_{off}(O_2)$ (s^{-1})	k_{on}(imidazole)[b] (mM^{-1} s^{-1})
*Bj*FixLH	218	140	0.14	20	16
*Ax*PDEA1H	212	12	6.7	77	1400
*Ec*DosH	nd[c]	13	0.0026	0.034	nd[c]
*Mt*DosH	217	2.0	6.0	12	74
*Rm*FixLH[e]	209	31	0.22	6.8	50
*Rm*FixLT[e]	209 (2.11 Å)[d]	50	0.22	11	37
SW Mb[f]	220 (2.11 Å)[d]	0.86	14	12	0.052

[a] All O_2 binding parameters (20−25 °C, pH 7.0−8.5) were previously reported (*6*, *9*, *12*). [b] Imidazole on-rate constants (pH 8.0, 25 °C) have been reported for only the FixL proteins and sperm whale myoglobin (*10*, *11*). [c] Not detected. [d] The value between the parentheses is the measured Fe−His bond length (*23*). [e] Tamura et al. (*18*). [f] Kitagawa et al. (*19*), Miyatake et al. (*23*), and Quillin et al. (*39*).

ν_{Fe-CO} frequencies covering many different heme proteins (Figure 4B) (*29*). ν_{C-O} and ν_{Fe-CO} of these heme proteins ranged from 1967 to 1973 cm^{-1} and from 487 to 497 cm^{-1}, respectively, and these values fall on the correlation line for imidazole coordination (Figure 4B), consistent with the amino acid sequence analysis (Figure 2B). This indicates that the axial ligand trans to the bound CO is a histidine residue in *Ec*Dos as well as in three other proteins. This has been confirmed by mutagenesis studies on histidine 77 (unpublished results of V. Delgado-Nixon and M.-A. Gilles-Gonzales). It is noted that ν_{C-O} and ν_{Fe-CO} of these heme proteins are perfectly normal and consistent with binding of CO to the heme without electrostatic interaction between the bound CO and amino acids in the distal pocket (*30*−*32*).

Shiro and co-workers have reported that ν_{Fe-CO} and ν_{C-O} of *S. meliloti* FixL are sensitive to the presence of the kinase domain, with ν_{Fe-CO} and ν_{C-O} being 502 and 1956 cm^{-1}, respectively, for the *Rm*FixLH heme-PAS and ν_{Fe-CO} and

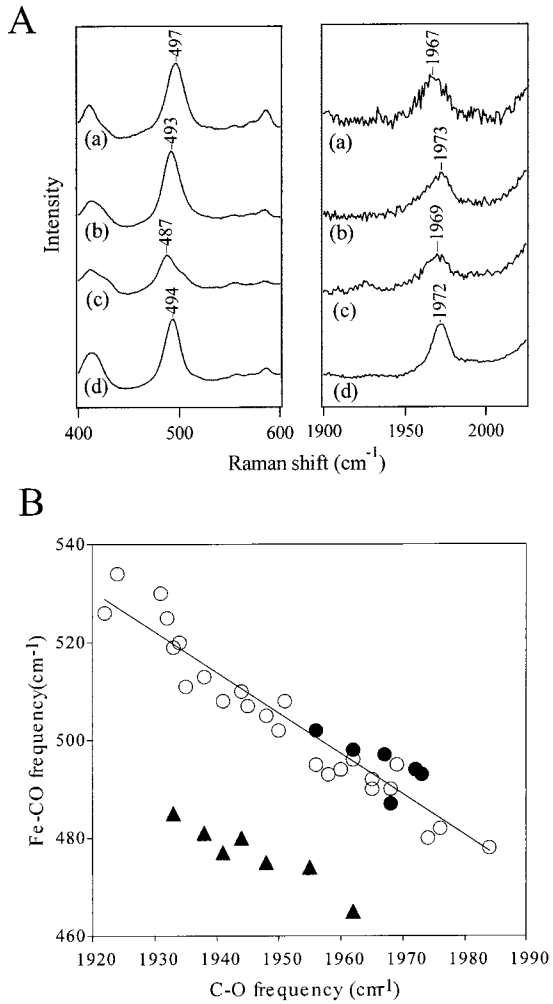

FIGURE 4: CO-bound heme-PAS proteins. Panel A shows 413.1 nm excited resonance Raman spectra of the carbonmonoxy forms of *Bj*FixLH (a), *Ax*PDEA1H (b), *Ec*DosH (c), and *Mt*DosH (d). The right and left panels show the low- and high-frequency regions of the spectra, respectively. Labeled peaks are assigend to the ν_{Fe-CO} and ν_{C-O} modes based on the results using ^{13}C isotope-substituted CO complexes. Panel B shows the inverse correlation between the ν_{Fe-CO} and ν_{C-O} frequencies. The filled circles are the heme-PAS proteins. The empty circles correspond to a variety of heme proteins with proximal histidine axial ligands. The triangles are for different cytochrome P450s that have cysteine as a proximal ligand. The data except for those for the heme-PAS proteins were taken from ref *29*.

Table 3: Resonance Raman Modes for O_2, CO, and NO Bound to Ferrous Heme-PAS

protein	ν_{Fe-O} (cm^{-1})	ν_{Fe-NO} (cm^{-1})	ν_{N-O} (cm^{-1})	ν_{Fe-CO}/ν_{C-O} (cm^{-1})	δ_{Fe-C-O} (cm^{-1})
*Bj*FixLH	569	568	1634	497/1967	574
*Bj*FixL	571	nd[c]	nd[c]	496/1969	571
*Ax*PDEA1H	567	560	1637	493/1973	581
*Ec*DosH	562	563	1632, 1576	487/1969	575
*Mt*DosH	573	567	1639	494/1972	570
*Rm*FixLH[a]	571	525, 558	1676	498/1962	576
*Rm*FixLT[a]	571	525, 558	1676	502/1956	572
SW Mb[b]	570	560	1613	512/1944	577

[a] Tamura et al. (*18*), Miyatake et al. (*23*), and Lukat-Rodgers and Rodgers (*25*). [b] Tomita et al. (*33*), Tsubaki et al. (*40*), and Van Wart and Zimmer (*41*). [c] Not detected.

ν_{C-O} being 498 and 1962 cm^{-1}, respectively, for the *Rm*FixLT kinase (*23*). They noted that a changed Fe−C−O bond angle in *Rm*FixLH (171°) compared to that in *Rm*FixLT (157°), found from EXAFS measurements, could account for the different Raman frequencies. Our results show that the Fe−CO and C−O stretches of the isolated *Bj*FixL heme-PAS and the complete *Bj*FixL enzyme are identical and are closer to the values obtained for the *Rm*FixLT enzyme than those of the isolated *Rm*FixLH heme-PAS (Table 3). Compared to carbonmonoxy-*Bj*FixLH, the Fe−C−O bending frequency of *Ax*PDEA1H was higher, and the ν_{Fe-CO} frequency was lower. These results indicate that the Fe−C−O bond angles increase in the following order: *Ax*PDEA1H < *Bj*FixLH < *Rm*FixLH.

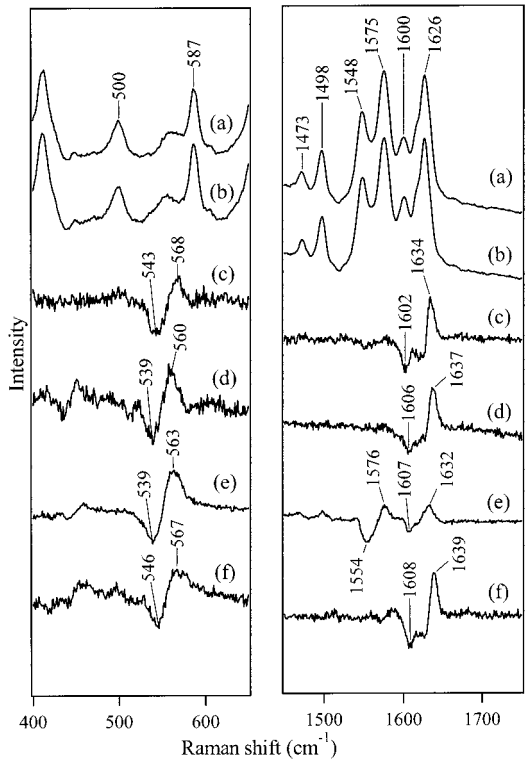

FIGURE 5: Resonance Raman spectra for the NO complexes of heme-PAS proteins with 413.1 nm excitation. Spectra of the ^{14}NO (a) and ^{15}NO (b) complexes of *Bj*FixLH are shown together with their difference spectrum (c) and the difference spectra for *Ax*PDEA1H (d), *Ec*DosH (e), and *Mt*DosH (f). The right and left panels show the low- and high-frequency regions, respectively.

Binding of NO. The low- and high-frequency region resonance Raman spectra for the NO complexes of ferrous *Bj*FixLH (a−c), *Ax*PDEA1H (d), *Ec*DosH (e), and *Mt*DosH (f) are shown in Figure 5 and summarized in Table 3. All of the NO adducts had Fe−NO stretching frequencies between 560 and 569 cm^{-1} and no additional isotope shift pattern in the 510−520 cm^{-1} region, clearly indicating hexacoordination of the heme iron and showing no sign of pentacoordination. In contrast, EPR spectra of the ferrous NO adduct of *Rm*FixLT showed a classic three-line nitrosyl heme signature at $g = 2.0$ consistent with as much as 50% of the signal arising from pentacoordinate nitrosyl heme (*10*, *18*, *27*). These differences may be explained by the unusually weak Fe−His bond of deoxy-*Rm*FixLT and by temperature-dependent variations in the penta- and hexacoordinate nitrosyl heme equilibrium for NO-*Rm*FixLT adducts (*27*, *34*). Electrostatic interactions of the bound NO with neighboring amino acid side chains would be expected to influence ν_{N-O}

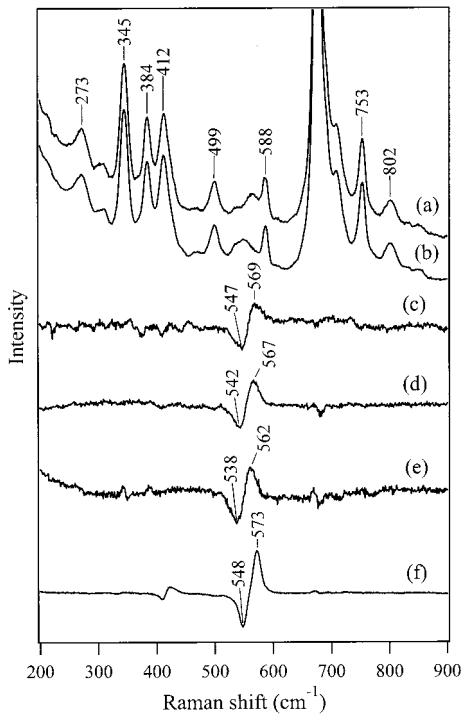

FIGURE 6: O_2-bound heme-PAS proteins. The resonance Raman spectra of [$^{16}O_2$]*Bj*FixLH (a) and [$^{18}O_2$]*Bj*FixLH (b) are followed by their $^{16}O_2 - {}^{18}O_2$ difference spectrum (c) (a − b) and the $^{16}O_2 - {}^{18}O_2$ difference spectra for the oxy forms of *Ax*PDEA1H (d), *Ec*DosH (e), and *Mt*DosH (f). The resonance Raman excitation was at 413.1 nm.

but not ν_{Fe-NO} (*34*). As such, the ν_{N-O} frequencies, ranging between 1634 and 1638 cm^{-1} for *Bj*FixL (c), *Ax*PDEA1H (d), and *Mt*DosH (f), are consistent with binding of NO in a hydrophobic cavity and without significant polar interactions. These results are also consistent with the ν_{C-O} behavior. Interestingly, we found *Ec*DosH (e) to have two conformations for its N−O stretch, with the frequency of one of them being remarkably low (1576 cm^{-1}). Such a low ν_{N-O} frequency is characteristic of the NO having a negative charge and being stabilized by strong hydrogen bonding (*34*). A highly bent structure of the bound Fe−N−O group would explain why NO, but not CO, engages in strong polar interactions with the *Ec*DosH heme pocket. Such a bent Fe−N−O structure has been reported for NO bound to ferrous *Bj*FixLH (*15*). Since the binding geometry of O_2 is assumed to be similar to that of NO, O_2 bound to *Ec*DosH would be expected to benefit from similar stabilizing interactions like NO. Candidates for stabilizing polar interactions in the *Ec*Dos distal pocket include the guanidinium side chain of arginine $G_\beta 2$ (Arg220 in *Bj*FixL) and the edge of the benzene ring of phenylalanine $H_\beta 4$ (Leu236 in *Bj*FixL) (Figure 2). Phenylalanine edges have been shown to stabilize polar ligands in several natural and mutant myoglobins, including elephant myoglobin (*29*, *35*).

Influence of the Heme Pocket Structure on Binding of O_2. Figure 6 shows the resonance Raman spectra for the O_2 adducts of the heme-PAS. The relatively high ν_{Fe-O} stretching frequency (573 cm^{-1}) of *Mt*DosH (f) is consistent with the 5−70-fold higher O_2 affinity of this protein (Figure 6 and Table 2). The quite low ν_{Fe-O} value (562 cm^{-1}) of oxy-*Ec*DosH (e) could be due to a steric effect on the bound O_2 (*36*−*38*). Heme-PAS proteins typically have extremely accessible, sterically unhindered heme pockets, as evidenced by their ν_{Fe-CO} frequencies and their rapid binding of imidazole (Tables 2 and 3). *Ec*Dos is the exception to this trend, showing no detectable tendency to bind imidazole. It is possible that the combination of a natural substitution of a phenylalanine at position $H_\beta 4$ (Leu236 in *Bj*FixL), together with a coordinating methionine at position FG8 (Ile218 in *Bj*FixL), leads to crowding of the heme distal pocket. Alternatively, the quite low ν_{Fe-O} frequency could be due to electrostatic interactions of the bound O_2 with the edge of the unique phenylalanine $H_\beta 4$ of *Ec*Dos (Figure 2). A 200−2000-fold lower off-rate constant for binding of O_2, compared to those of the other heme-PASs, also suggests the *Ec*DosH heme pocket features additional stabilizing interactions with O_2 (Table 2).

Concluding Remarks. The heme-PAS proteins represent a large class of sensory hemes, occurring in quite different organisms and regulating different enzymatic activities as part of their function in signal transduction. Given the relatively small sampling of heme-PAS proteins and the already significant range of heme coordination and ligand binding properties, this class of signal-transducing proteins is likely to be at least as diverse as the hemoglobins. Very few trends apply to the entire family of heme-PAS proteins. Therefore, it is important not to try to infer the behavior for one member, even another FixL protein, from observations of *S. meliloti* FixL. A surprising finding from this comparative resonance Raman study is the range of ν_{Fe-His} frequencies for these proteins, which is quite broad (209−217 cm^{-1}) and not indicative of heme reactivity or even Fe−His bond length (Table 2). Another unexpected finding is that, compared to most of the heme-PAS distal pockets, which are hydrophobic and unhindered, the *Ec*Dos heme pocket is relatively complex. This heme pocket features at least one additional barrier to ligand binding in its endogenous sixth axial ligand and provides at least one additional stabilizing interaction with bound O_2 or NO.

ACKNOWLEDGMENT

We thank Dr. T. Kitagawa for the use of his Raman facilities and Mr. Elhadji M. Dioum for technical assistance.

REFERENCES

1. Taylor, B. L., and Zhulin, I. B. (1999) *Microbiol. Mol. Biol. Rev. 63*, 479−506.
2. Gilles-Gonzalez, M. A. (2001) *IUBMB Life 51*, 165−173.
3. Gilles-Gonzalez, M. A., Ditta, G. S., and Helinski, D. R. (1991) *Nature 350*, 170−172.
4. Gilles-Gonzalez, M. A., Gonzalez, G., and Perutz, M. F. (1995) *Biochemistry 34*, 232−236.
5. Tuckerman, J. R., Gonzalez, G., and Gilles-Gonzalez, M. A. (2001) *J. Mol. Biol. 308*, 449−455.
6. Chang, A. L., Tuckerman, J. R., Gonzalez, G., Mayer, R., Weinhouse, H., Volman, G., Amikam, D., Benziman, M., and Gilles-Gonzalez, M. A. (2001) *Biochemistry 40*, 3420−3426.
7. Gong, W., Hao, B., Mansy, S. S., Gonzalez, G., Gilles-Gonzalez, M. A., and Chan, M. K. (1998) *Proc. Natl. Acad. Sci. U.S.A. 95*, 15177−15182.
8. Miyatake, H., Mukai, M., Park, S.-Y., Adachi, S.-I., Tamura, K., Nakamura, H., Nakamura, K., Tsuchiya, T., Iizuka, T., and Shiro, Y. (2000) *J. Mol. Biol. 301*, 415−431.
9. Gilles-Gonzalez, M. A., Gonzalez, G., Perutz, M. F., Kiger, L., Marden, M. C., and Poyart, C. (1994) *Biochemistry 33*, 8067−8073.

10. Winkler, W. C., Gonzalez, G., Wittenberg, J. B., Hille, R., Dakappagari, N., Jacob, A., Gonzalez, L. A., and Gilles-Gonzalez, M. A. (1996) *Chem. Biol. 3*, 841−850.
11. Mansy, S. S., Olson, J. S., Gonzalez, G., and Gilles-Gonzalez, M. A. (1998) *Biochemistry 37*, 12452−12457.
12. Delgado-Nixon, V. M., Gonzalez, G., and Gilles-Gonzalez, M. A. (2000) *Biochemistry 39*, 2685−2691.
13. Bertolucci, C., Ming, L.-J., Gonzalez, G., and Gilles-Gonzalez, M. A. (1996) *Chem. Biol. 3*, 561−566.
14. Monson, E. K., Ditta, G. S., and Helinski, D. R. (1995) *J. Biol. Chem. 270*, 5243−5250.
15. Gong, W., Hao, B., and Chan, M. K. (2000) *Biochemistry 39*, 3955−3962.
16. David, M., Daveran, M.-L., Batut, J., Dedieu, A., Domergue, O., Ghai, J., Hertig, C., Boistard, P., and Kahn, D. (1988) *Cell 54*, 671−683.
17. Ditta, G., Virts, E., Palomares, A., and Kim, C.-H. (1987) *J. Bacteriol. 169*, 3217−3223.
18. Tamura, K., Nakamura, H., Tanaka, Y., Oue, S., Tsukamoto, K., Nomura, M., Tsuchiya, T., Adachi, S., Takahashi, S., Iizuka, T., and Shiro, Y. (1996) *J. Am. Chem. Soc. 118*, 9434−9435.
19. Kitagawa, T., Nagai, K., and Tsubaki, M. (1979) *FEBS Lett. 104*, 376−378.
20. Nagai, K., Kitagawa, T., and Morimoto, H. (1980) *J. Mol. Biol. 136*, 271−289.
21. Matsukawa, S., Mawatari, K., Yoneyama, Y., and Kitagawa, T. (1985) *J. Am. Chem. Soc. 107*, 1108−1113.
22. Ross, P., Mayer, R., and Benziman, M. (1991) *Microbiol. Rev. 55*, 35−58.
23. Miyatake, H., Mukai, M., Adachi, S., Nakamura, H., Tamura, K., Iizuka, T., Shiro, Y., Strange, R. W., and Hasnain, S. S. (1999) *J. Biol. Chem. 274*, 23176−23184.
24. Rodgers, K. R., Lukat-Rodgers, G. S., and Barron, J. A. (1996) *Biochemistry 35*, 9539−9548.
25. Lukat-Rodgers, G. S., and Rodgers, K. R. (1997) *Biochemistry 36*, 4178−4187.
26. Rodgers, K. R., Lukat-Rodgers, G. S., and Tang, L. (1999) *J. Am. Chem. Soc. 121*, 11241−11242.
27. Rodgers, K. R., Lukat-Rodgers, G. S., and Tang, L. (2000) *J. Biol. Inorg. Chem. 5*, 642−654.
28. Spiro, T. G., and Li, X.-Y. (1988) in *Biological Applications of Raman Spectroscopy* (Spiro, T. G., Ed.) Vol. III, pp 1−37, Wiley, New York.
29. Das, T. K., Wilson, E. K., Cutruzzolà, F., Brunori, M., and Rousseau, D. L. (2001) *Biochemistry 40*, 10774−10781.
30. Li, T., Quillin, M. L., Phillips, G. N., Jr., and Olson, J. S. (1994) *Biochemistry 33*, 1433−1446.
31. Phillips, G. N., Jr., Teodoro, M., Li, L., Smith, B., Gilson, M. M., and Olson, J. S. (1999) *J. Phys. Chem. B 103*, 8817−8829.
32. Ray, G. B., Li, X.-Y., Ibers, J. A., Sessler, J. L., and Spiro, T. G. (1994) *J. Am. Chem. Soc. 116*, 162−176.
33. Tomita, T., Hirota, S., Ogura, T., Olson, J. S., and Kitagawa, T. (1999) *J. Phys. Chem. B 103*, 7044−7054.
34. Park, E.-S., Thomas, M. R., and Boxer, S. G. (2000) *J. Am. Chem. Soc. 122*, 12297−12303.
35. Hirota, S., Li, T., Philips, G. N., Jr., Olson, J. S., Mukai, M., and Kitagawa, T. (1996) *J. Am. Chem. Soc. 118*, 7845−7846.
36. Mukai, M., Nakamura, K., Nakamura, H., Iizuka, T., and Shiro, Y. (2000) *Biochemistry 39*, 13810−13816.
37. Das, T. K., Weber, R. E., Dewilde, S., Wittenberg, J. B., Wittenberg, B. A., Yamauchi, K., Van Hauwaert, M.-L., Moens, L., and Rousseau, D. L. (2000) *Biochemistry 39*, 14330−14340.
38. Yeh, S.-R., Couture, M., Ouellet, Y., Guertin, M., and Rousseau, D. L. (2000) *J. Biol. Chem. 275*, 1679−1684.
39. Quillin, M. L., Arduini, R. M., Olson, J. S., and Phillips, G. N., Jr. (1993) *J. Mol. Biol. 234*, 140−155.
40. Tsubaki, M., Srivastava, R. B., and Yu, N.-T. (1982) *Biochemistry 21*, 1132−1140.
41. Van Wart, H. E., and Zimmer, J. (1985) *J. Biol. Chem. 260*, 8372−8377.

BI0158831